PHYSICAL REVIEW D **90,** 125010 (2014)

Equation of state of two-dimensional Yang-Mills theory

Nikhil Karthik* and Rajamani Narayanan†
Department of Physics, Florida International University, Miami, Florida 33199, USA
(Received 12 November 2014; published 15 December 2014)

We study the pressure, P, of SU(N) gauge theory on a two-dimensional torus as a function of area, $A = l/t$. We find a crossover scale that separates the system on a large circle from a system on a small circle at any finite temperature. The crossover scale approaches zero with increasing N and the crossover becomes a first-order transition as $N \to \infty$ and $l \to 0$ with the limiting value of $\frac{2Pl}{(N-1)t}$ depending on the fixed value of Nl.

DOI: 10.1103/PhysRevD.90.125010 PACS numbers: 11.15.-q, 11.10.Wx

I. INTRODUCTION

The partition function for SU(N) gauge theory on a 2D torus with spatial extent l and temperature t is only a function of the area, $A = l/t$, and is given by [1]

$$Z_N(A) = \sum_r \exp\left(-\frac{C_r^{(2)} l}{Nt}\right), \tag{1}$$

where $C_r^{(2)}$ is the value of Casimir in the representation r. One can arrive at Eq. (1) by taking the continuum limit of a lattice formalism on a finite lattice [2]. The asymptotic behavior at large N was studied in [3] where only representations with $C_r^{(2)}$ of $\mathcal{O}(N)$ dominate. Since the partition function is a sum over stringlike states with energies proportional to the spatial extent, l, the pressure given by

$$P \equiv t\frac{\partial}{\partial l}\ln Z = \frac{\partial}{\partial A}\ln Z = -\frac{1}{N}\langle C_r^{(2)}\rangle, \tag{2}$$

is negative.

The partition function for SU(2) is simple and is given by

$$Z = \sum_{\lambda=0}^{\infty} e^{-\frac{(\lambda^2+2\lambda)A}{4}} = \frac{1}{2}e^{\frac{A}{4}}\left[\sum_{\lambda=-\infty}^{\infty} e^{-\frac{\lambda^2 A}{4}} - 1\right]$$
$$= \frac{1}{2}e^{\frac{A}{4}}\left[\sqrt{\frac{4\pi}{A}}\sum_{\lambda=-\infty}^{\infty} e^{-\frac{4\pi^2\lambda^2}{A}} - 1\right]. \tag{3}$$

The asymptotic behavior of the equation of state is

$$\frac{Pl}{t} = -\frac{3}{4}\frac{l}{t}e^{-\frac{3l}{4t}} \quad \text{as } l \to \infty, \tag{4}$$

and

$$\frac{Pl}{t} = -\frac{1}{2} \quad \text{as } l \to 0. \tag{5}$$

The behavior at large l is dominated by a few low-lying energy states, whereas the behavior at small l comes from a sum over all states and could be interpreted as the equipartition limit with the number of degrees of freedom being 1 for SU(2). The crossover from the behavior on a large circle to a small circle is shown in Fig. 1.

Expecting that the equipartition limit is given by

$$\frac{Pl}{t} = -\frac{N-1}{2} \quad \text{as } l \to 0, \tag{6}$$

for all N, we define

$$Q(\alpha) \equiv -\frac{2Pl}{(N-1)t}; \quad \text{with} \quad \alpha = \frac{Nl}{t}, \tag{7}$$

and study this quantity in this paper.

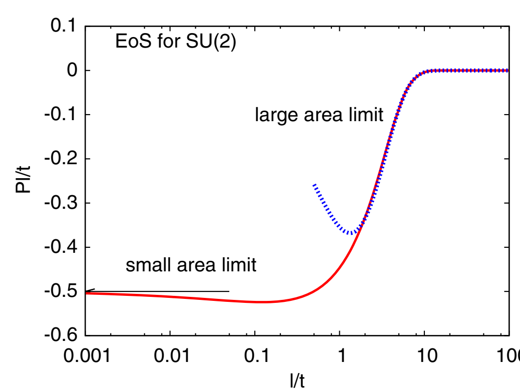

FIG. 1 (color online). The equation of state for SU(2) gauge theory on a two-dimensional torus is shown as the solid curve. The asymptotic values of Pl/t at small area is -0.5. At very large area, Pl/t behaves as $0.75\exp(-0.75l/t)l/t$, which is shown as the dotted curve. There is a crossover between the two limits.

*nkarthik@fiu.edu
†rajamani.narayanan@fiu.edu

II. SUMMARY OF RESULTS

We will show the following results in this paper using a numerical simulation of the partition function in Eq. (1):

(1) $Q(\alpha)$ falls on a universal curve as $N \to \infty$.

(2) $Q(\alpha)$ goes to zero as α goes to infinity. This result implies that the pressure at infinite N is zero for all l at any t as long as one takes $N \to \infty$ keeping l and t finite, and is consistent with physics being independent of temperature and spatial extent in the infinite-N limit [4,5].

(3) $Q(\alpha)$ goes to unity as α goes to zero. This limit is reached from a finite l and t only at finite N.

(4) There is a crossover point defined as a peak in the susceptibility,

$$\chi = A\frac{\partial}{\partial A}Q = \alpha\frac{\partial}{\partial \alpha}Q. \tag{8}$$

(a) The large l side of the crossover is dominated by representations where $C_r^{(2)}$ are of $\mathcal{O}(N)$. This is the case of interest for all nonzero l at infinite N and was studied in [3].

(b) The small l side of the crossover is dominated by representations where $C_r^{(2)}$ are of $\mathcal{O}(N^2)$.

(5) Since the value of Q at infinite N and $l = 0$ (or equivalently $t = \infty$) depends on the approach to the limit, $N \to \infty$ and $l \to 0$, there is a first-order transition confirming the argument in [6].

III. PROPERTIES OF CASIMIR FOR SU(N)

The representations of SU(N) are specified by the sequence of integers $\Lambda_r = (\lambda_1, \lambda_2, \ldots, \lambda_{N-1})$, subjected to the ordering $\lambda_i \geq \lambda_{i+1}$, and the value of $C_r^{(2)}$ is

$$C_r^{(2)} = \sum_{i=1}^{N-1}\lambda_i^2 - \sum_{i=1}^{N-1} i\lambda_i - \frac{\lambda^2}{N} + (N+1)\lambda \quad \text{where } \lambda = \sum_{i=1}^{N-1}\lambda_i. \tag{9}$$

The maximum and minimum values of Casimir, given the constraint that λ has to be kept fixed, will be used in the subsequent sections. The representation with the maximum value of $C_r^{(2)}$ for a given λ is given by

$$\Lambda_{\max} = (\lambda, 0, \ldots, 0). \tag{10}$$

The minimum value of $C_r^{(2)}$ is given by the sequence $\Lambda_{\min}$,

$$\lambda_i = \begin{cases} \lfloor\frac{\lambda}{N-1}\rfloor + 1 & \text{if } i \leq k \equiv \lambda - (N-1)\lfloor\frac{\lambda}{N-1}\rfloor \\ \lfloor\frac{\lambda}{N-1}\rfloor & \text{if } i > k. \end{cases} \tag{11}$$

To prove that the two sequences extremize the Casimir, note that the Casimir decreases under the transformation $(\lambda_1, \lambda_2, \ldots, \lambda_i, \ldots, \lambda_j, \ldots, \lambda_{N-1})$ to $(\lambda_1, \lambda_2, \ldots, \lambda_i - 1, \ldots, \lambda_j + 1, \ldots, \lambda_{N-1})$ for $j > i$, provided this transformation is allowed. Such a transformation is not possible for $\Lambda_{\min}$. Similarly, the reverse of that transformation is not possible on $\Lambda_{\max}$. One can prove by contradiction that $\Lambda_{\min}$ and $\Lambda_{\max}$ uniquely satisfy these properties.

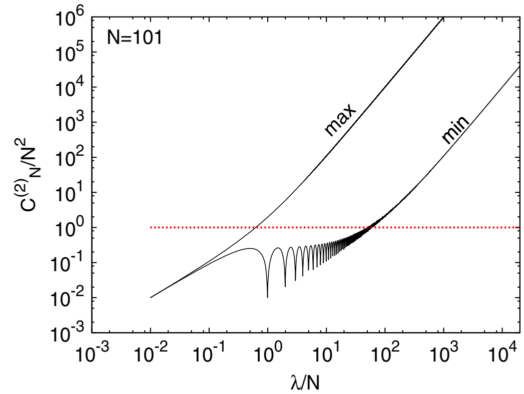

FIG. 2 (color online). Behavior of Casimir as a function of λ. The upper solid curve is the maximum value of Casimir given a value of λ, as a function of λ. Similarly, the lower solid curve is the minimum value of Casimir given a value of λ, as a function of λ. The dotted line is where $C_r^{(2)} = N^2$.

We have shown the behavior of the maximum and minimum values of $C_r^{(2)}$ as a function of λ in Fig. 2. The minimum of $C_r^{(2)}$ shows a quasiperiodic behavior, with troughs at $\lambda = qN$ for integer q. The values of Casimir at these troughs are

$$C_{\min} = N\left(1 + \lfloor\frac{q}{N-1}\rfloor\right)\left(2q - \lfloor\frac{q}{N-1}\rfloor(N-1)\right), \tag{12}$$

whose dependence on N is linear for q between two multiples of $(N-1)$ and is quadratic for q that are multiples of $(N-1)$. On very large circles (or at very low temperatures), one would expect that only the excitations around these troughs at small q would be important. On very small circles (or at very high temperatures), large values of q would become accessible, where all possible Casimir are $\mathcal{O}(N^2)$. This is the region above the red dotted line in Fig. 2 where $C_r^{(2)}$ is larger than N^2. Qualitatively, this is the difference one might expect between the low- and high-temperature phases.

IV. HEAT-BATH ALGORITHM

We simulated the partition function in Eq. (1) by updating Λ_r with the heat-bath algorithm. Each heat-bath update is a sequence of local updates from λ_1 to λ_{N-1}, in that order, such that the ordering of λ_i is preserved. For the local update of λ_i, the probability distribution of λ_i is given by a discrete version of the Gaussian distribution

$$T(\lambda_i) \propto e^{-(\lambda_i - \mu_i)^2/2\sigma^2}, \tag{13}$$

subject to the condition $\lambda_{i+1} \leq \lambda_i \leq \lambda_{i-1}$ for $i > 1$ and $\lambda_2 \leq \lambda_1$. The μ_i and σ_i for the above discrete Gaussian distribution are functions of the rest of the λ_i's forming the heat bath,

$$\mu_i = \frac{\bar{\lambda} + N(\frac{2i-N-1}{2})}{N-1} \quad \text{and} \quad \sigma^2 = \frac{N^2}{2A(N-1)}, \qquad (14)$$

where $\bar{\lambda} = \sum_{j \neq i} \lambda_j$. For $i > 1$, the set of allowed values for λ_i is bounded from above and below. Hence, we included all the allowed possibilities weighted by Eq. (13) as candidates for the update. Since Eq. (14), along with the inequality $\lambda - \lambda_1 < (N-2)\lambda_2$, implies that $\mu_1 < \lambda_2$, the probability for λ_1 is a monotonically decreasing function. This enables one to put an upper cutoff on λ_1. In our calculation, we used an upper cutoff of $\lambda_2 + 3\sigma$. We also checked that changing this value to $\lambda_2 + 10\sigma$ does not cause any statistically significant changes. Since a representation r and its conjugate representation $\bar{r}$ have the same Casimir, one can do an over-relaxation step by a global update $\lambda'_i = \lambda_1 - \lambda_{N-i+1}$.

In our simulations, the successive measurements were separated by 100 iterations of 2 heat-bath and 1 over-relaxation steps. The first 2000 measurements were discarded for thermalization. In this way, we collected 10^4 configurations of Λ_r at all area and N.

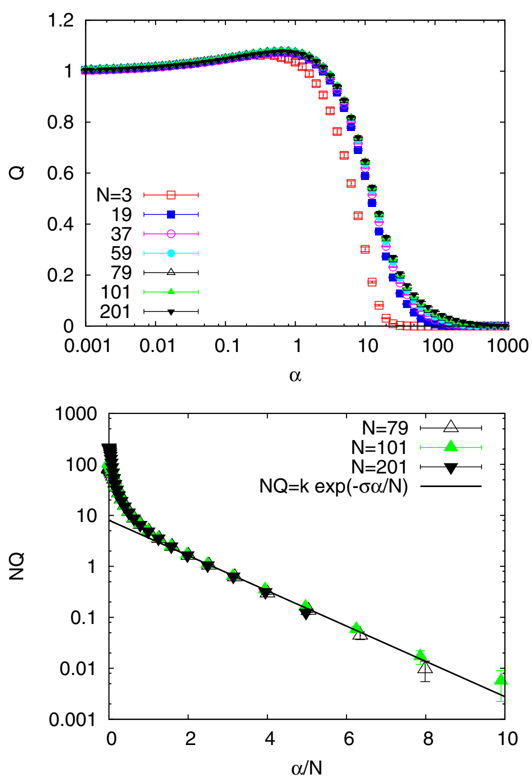

FIG. 3 (color online). Q as a function of the scaled area $\alpha = NA$ is shown in the top panel. It is seen that Q as a function of α has a large-N limit. For very small values of α, Q approaches 1. In the bottom panel, the large area behavior of Q in the large-N limit is shown. In this case, QN behaves as $\exp(-\sigma\alpha/N)$.

V. RESULTS

In the top panel of Fig. 3, we show the behavior of Q as a function of the scaled area α for various values of N. The important thing to notice is that Q has a large-N limit when plotted as a function of α. For $\alpha \ll 1$, Q seems to approach 1 for all N. This is in agreement with our intuition based on the equipartition theorem. The nontrivial observation is that this crossover to the equipartition limit happens at a finite value of α in the large-N limit. For $\alpha \gg 1$, Q seems to behave as $N^{-1}\exp(-\sigma\alpha/N)$ for a constant $\sigma \approx 0.81$ in the large-N limit. This is shown in the bottom panel of Fig. 3. Thus, it can also be seen as a crossover from the strong-coupling regime, which has a scale σ, to the weak-coupling regime with no underlying scale.

We determined the crossover point α_c using the peak position of the susceptibility χ, after interpolating using multihistogram reweighting. We show χ as a function of α in Fig. 4 for various N. The susceptibility also has a large-N limit when plotted as a function of α. The peak positions of susceptibility for $N > 19$ agree within errors, giving us an estimate $\alpha_c = 12.1(2)$. This implies that the crossover area $A_c = \alpha_c/N$ shifts to smaller values at larger N. The width of the susceptibility when expressed in terms of the area A decreases inversely as N. This is characteristic of finite volume scaling near a first-order phase transition, with the large-N limit replacing the thermodynamic limit in this case.

The reason for this crossover can be understood from the scatter plot of $C_r^{(2)}$ versus λ measured during the course of the Monte Carlo run using a value of α. Such scatter plots at various α are shown in Fig. 5 for two different N. We also show the maximum and minimum values of Casimir at a fixed λ, as a function of λ. As discussed earlier, the minimum Casimir shows a quasiperiodic behavior, forming wells with a periodicity N. At large values of α, the

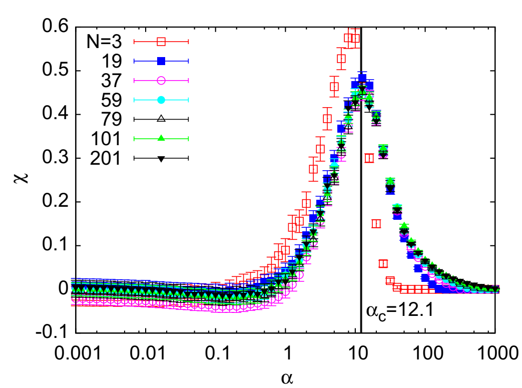

FIG. 4 (color online). Susceptibility χ as a function of the scaled area $\alpha = NA$. The crossover coupling α_c is shown by the vertical line.

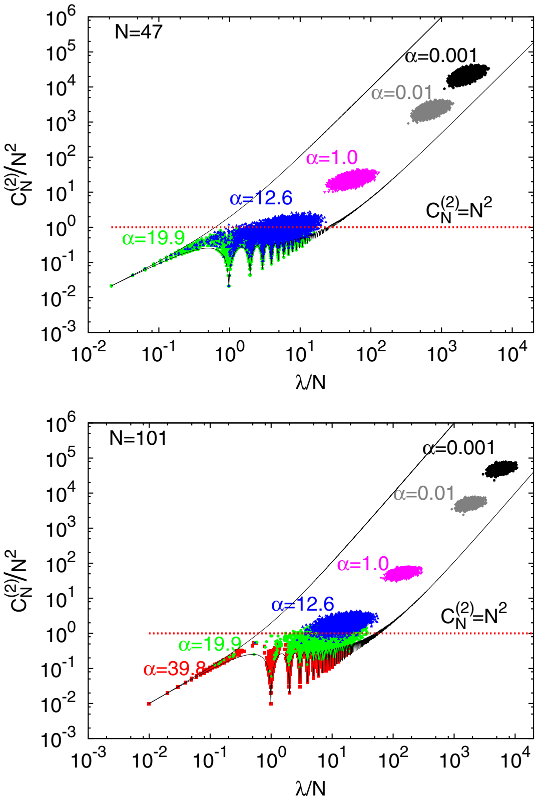

FIG. 5 (color online). Scatter plot of $C_r^{(2)}/N^2$ versus λ/N at various area A. The top panel is for $N = 47$ and the bottom for $N = 101$. Each point corresponds to a $C_r^{(2)}$ and λ measured in the course of a Monte Carlo simulation at a particular α specified by the color. The upper and lower solid curves are the maximum and minimum values of $C_r^{(2)}$ at a given λ, respectively.

representations near the troughs of these wells at small values of λ get populated. The representations within these wells are sparse, and this discreteness governs the large area behavior. At very small area, the most probable $C_r^{(2)}$ moves away from the line of minimum $C_r^{(2)}$ and remains in a region where one can approximate the distribution of Casimir by a continuum. The crossover between the two behaviors is what shows up as a peak in χ. As discussed in Sec. III, the Casimir near the troughs at small λ is of $\mathcal{O}(N)$, while the Casimir at very large λ is of $\mathcal{O}(N^2)$. As shown by the dotted line in Fig. 5, this crossover at $\alpha \approx 12.1$ roughly occurs when the dominant behavior $C_r^{(2)}$ changes from $\mathcal{O}(N)$ to $\mathcal{O}(N^2)$.

VI. CONCLUSIONS

Yang-Mills theory in two dimensions is always in the confined phase. We focused on the quantity, $Q = -\frac{2Pl}{(N-1)t}$, to study the equation of state. We showed that the equation of state shows a crossover from strong coupling (large spatial extent) to weak coupling (small spatial extent) within the confined phase. Viewed as a function of $\alpha = \frac{lN}{t}$, $Q(\alpha)$ approaches a universal curve as $N \to \infty$ as

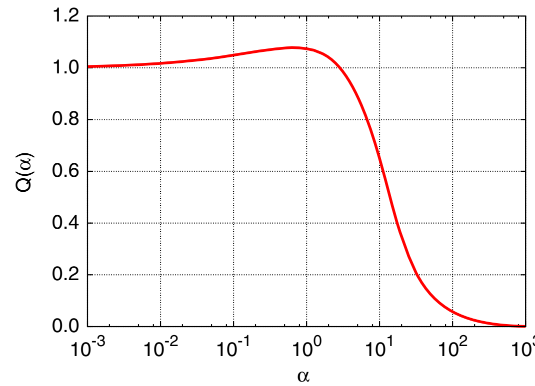

FIG. 6 (color online). The large-N limit of Q as a function of α.

shown in Fig. 6. This behavior is similar to the Durhuus-Olesen transition [7,8] with the double scaling limit for the equation of state being $N \to \infty$ and $l \to 0$ (or $t \to \infty$), keeping $\alpha = \frac{lN}{t}$ fixed. There is a line of crossover, $\frac{lN}{t} = \alpha_c$, extending from the origin in the $\frac{l}{t} - \frac{1}{N}$ diagram as shown in Fig. 7. Well above this line, $Q \ll 1$, and it behaves as $\exp(-\sigma A)/N$. Well below this line, Q is approximately 1. Depending on the slope, α, of the line along which the $N \to \infty$ and $\frac{l}{t} \to 0$ limit is taken, the limiting value of Q differs. Specifically, if the $N \to \infty$ limit is taken after the $A \to 0$ limit is taken, then Q is 1. When the two limits are reversed, Q becomes 0. Therefore, the crossover along $AN = \alpha_c$ becomes a first-order transition at vanishing area in the large-N limit.

The equation of state in four-dimensional Yang-Mills theories for several different values of N has been recently studied [9]. The pressure is found to be close to zero in the confined phase. In light of this paper, it would be

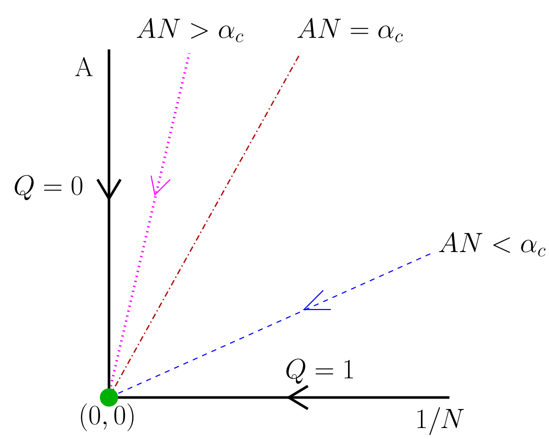

FIG. 7 (color online). Phase diagram. Various approaches to vanishing area at large N are indicated by lines with arrows. The critical value of the slope $AN = \alpha_c$ is shown as the dot-dashed line. For values of $AN \gg \alpha_c$ (the dotted line), Q decays exponentially with area. For values of $AN \ll \alpha_c$ (the dashed line), $Q \approx 1$. In particular, when A is reduced to 0 after taking the large-N limit (i.e., along the y axis), Q vanishes. When the two limits are interchanged (i.e., along the x axis), Q becomes 1.

interesting to perform a careful study of the equation of state in the confined phase in three and four dimensions and see if one can see a crossover similar to the one seen here in two dimensions.

ACKNOWLEDGMENTS

The authors acknowledge partial support by the NSF under Grant No. PHY-1205396.

[1] A. A. Migdal, Sov. Phys. JETP **42**, 413 (1975).

[2] J. Kiskis, R. Narayanan, and D. Sigdel, Phys. Rev. D **89**, 085031 (2014).

[3] D. J. Gross and W. Taylor, Nucl. Phys. **B400**, 181 (1993).

[4] D. Gross and E. Witten, Phys. Rev. D **21**, 446 (1980).

[5] T. Eguchi and H. Kawai, Phys. Rev. Lett. **48**, 1063 (1982).

[6] L. D. McLerran and A. Sen, Phys. Rev. D **32**, 2794 (1985).

[7] B. Durhuus and P. Olesen, Nucl. Phys. **B184**, 461 (1981).

[8] R. Narayanan and H. Neuberger, J. High Energy Phys. 12 (2007) 066.

[9] S. Datta and S. Gupta, Phys. Rev. D **82**, 114505 (2010).